Effect of doping (TMTSF)2ClO4 with TMTTF - I. Ambient pressure results : a competition between the different possible ground states

C. Coulon, P. Delhaes, J. Amiell, J.P. Manceau, J.M. Fabre, L. Giral

J. Physique **43** (1982) 1721-1729 NOVEMBRE **1982,** PAGE 1721

Classification
Physics Abstracts
64.70K — 71.30

Effect of doping $(TMTSF)_2ClO_4$ with TMTTF
I. Ambient pressure results : a competition between the different possible ground states

C. Coulon, P. Delhaes, J. Amiell, J. P. Manceau, J. M. Fabre (*) and L. Giral (*)

Centre de Recherches Paul Pascal, Domaine Universitaire, 33405 Talence, France

(*) Laboratoire de Chimie Structurale Organique (USTL), 34060 Montpellier, France

(*Reçu le 23 mars 1982, révisé le 26 juillet, accepté le 27 juillet 1982*)

Résumé. — Nous décrivons les propriétés de transport et les résultats de l'étude RPE d'échantillons de $(TMTSF)_2ClO_4$ dopés avec du TMTTF. Le rôle du dopage sur le comportement métallique à haute température est présenté et analysé ; cependant, l'essentiel du travail est dévolu au comportement basse température. La phase supraconductrice 3d qui existe à 1 K à pression ambiante dans le sel de TMTSF disparaît rapidement et le dopage favorise l'apparition d'une phase isolante à basse température. L'évolution des caractéristiques de cette phase avec le dopage est interprétée comme liée au passage d'un état d'onde de spin à un état non magnétique ; un modèle phénoménologique est discuté pour rendre compte de ces résultats.

Abstract. — We report on transport and EPR studies of $(TMTSF)_2ClO_4$ doped with TMTTF. The role of doping by the sulphur analog on the high temperature metallic range is presented and discussed; nevertheless a large part of this work is devoted to the low temperature behaviour. The 3d superconductive phase which occurs around 1 K under ambient pressure in the pure TMTSF salt is shown to be quickly suppressed. The doping process favours the stabilization of an insulating phase at low temperature and the change with increasing doping of the magnetic properties is explained as a cross-over from a SDW to a non-magnetic ground state; a phenomenological model is discussed to support these experimental results.

Since the discovery of the superconductivity of $(TMTSF)_2PF_6$ (*bis* tetramethyltetraselenafulvalene hexafluorophosphate) under pressure [1], extensive research have been devoted to the TMTSF radical-cations family revealing particularly striking physical properties. Among them, should be noted the high electrical conductivity in the metallic regime [2] and the nature of the low temperature phase transitions. Besides the order-disorder phase transitions involving the anions [3, 4], the 1d interacting electronic gas does not show the usual charge density wave instability (CDW) [5] but is governed by the competition between spin density wave (SDW) and superconductive (SC) ground states [6].

At first sight, the TMTTF (*bis* tetramethyltetrathiafulvalene) analogs of these salts although isomorphous to the TMTSF compounds [7] behave absolutely differently at ambient pressure; they are poor conductors and show a broad maximum of electrical conductivity at high temperatures (except the bromine salt) [8, 9]. However, a more detailed study reveals some characteristic features for these compounds [9]. Either the order-disorder phase transitions take place for the low-symmetrical anions [5, 9] or the intrinsic metal-insulator phase transitions occur at very low temperatures (approximatively the same as for the metal-SDW transition of $(TMTSF)_2PF_6$ at ambient pressure : T_c = 12 K). EPR studies have shown that this ground state is non-magnetic for the PF_6 salt [9], but the antiferromagnetic nature of the low temperature phase of the bromine compound has been recently revealed by NMR and antiferromagnetic resonance [10, 11]. Moreover, the PF_6 salt shows a weak « $2k_F$ » superstructure below the metal-insulator transition for which the 1d nature of the pretransitional diffusion has been demonstrated [5]. From a theoretical point of view, the low temperature ground state of $TMTTF_2PF_6$ has been described by Emery *et al.* [12] as a Spin Peierls (SP) ground state whose stabilization is governed by the growth of a 4 k_F

charge density wave at higher temperature. This 4 k_F CDW does not change the symmetry of the system and is equivalent to a localization of the electrons [12].

Finally for $(TMTTF)_2Br$, superconducting properties under a high pressure have also been reported [12].

Thus, a unique phase diagram for both the TMTSF and TMTTF series could be suspected. To obtain experimental confirmation of this conjoncture, one possibility is to study the magnetic character of the metal-insulator transition of the TMTTF salts under pressure. This study cannot be carried out with only electrical conductivity measurements since the behaviour of the resistivity is similar for the SP or SDW ground states; therefore magnetic measurements such as NMR or EPR under pressure are necessary. Because of the difficulty in carrying out such experiments, other experimental approaches are clearly useful. One of them is the synthesis of alloys starting from TMTTF and TMTSF salts. The physical properties of $|(TMTSF)_{1-x}(TMTTF)_x|_2PF_6$ salts for several values of x has already been reported [14].

In this paper, we present the study of $(TMTSF)_2ClO_4$ crystals doped with TMTTF. Because of the superconducting properties of $(TMTSF)_2ClO_4$, the effect of the doping on both the superconductive instability and the insulating phases can be investigated. The paper will be restricted to the ambient pressure results. The effect of pressure will be discussed in a following publication (part. 2 of this work).

1. **Synthesis and characterization of the samples.** — The samples were prepared by an electrochemical method already described by Bechgaard *et al.* [2], the applied voltage is kept constant at 0.4 V during the growth of the crystals, this value being intermediate between the first oxidation potentials of the two species, in the employed solvent 1-1'-2-trichloroethane. Usually, the crystals grow during about 24 hours. The electrooxidation yield is about 25 to 40 % which means that the larger part of the parent molecules TMTTF/TMTSF is left in the solvent.

The characterization of the samples was made using electronic microprobe spectroscopy and X-ray emission for sulphur (K line) and selenium (L line). Testing several parts of a crystal along the needle axis and a few crystals within a batch allows us to estimate the spread of homogeneity for the different samples. By this method the mean value $\bar{x}$ and the standard deviation Δx of the measured TMTTF concentration can be given. These values are summarized in table I. A further confirmation will be obtained from the unit cell determination on these samples [15].

In definitive, this analysis allows us to classify the different compounds even if Δx gives only an upper limit for a measure of their inhomogeneity (the quality of the crystal surface and the detector noise implies an enhancement of Δx). Furthermore it is noteworthy to indicate that the initial concentration of TMTTF in the prepared solution for the electrooxidation technique is, in any case, much more larger than the mean concentration $\bar{x}$ obtained inside the solid and reported in table I. Typically, the ratio between the solution values and the crystal values is between 3 and 5. This discrepancy is due to the TMTTF and TMTSeF solubility difference in 1-1'-2-trichloroethane. This point explains the difficulties in making solid solutions which are rich in TMTTF.

2. **Experimental investigations on transport and magnetic properties.** — 2.1 ELECTRICAL CONDUCTIVITY MEASUREMENTS. — The longitudinal electrical conductivity σ'' was measured for the different samples using the standard four probe a.c. method.

The room temperature values are reported in figure 1 on which we also give the results of Mortensen *et al.* concerning the PF_6 alloys [14]. Both results are consistent. They indicate a strong decrease of σ'' (300 K) even for the small values of x.

We have also studied the temperature dependence of the longitudinal conductivity for the different samples.

Concerning the lightest doped alloys (1), (2), (3), a very low temperature range has been explored using a ^3He-^4He dilution refrigerator. During the temperature lowering, the resistivity measurements have

Table I. — *Reference of the different alloys investigated in this paper and some of their physical characteristics : mean value and standard deviation of x, T_c values for the metal-insulator transition from σ'' and* EPR *and T_c' for the superconductive phase transition.*

Reference of the alloys	$(\bar{x} \pm \Delta x)$ %	T_c (K) from $\sigma(T)$	T_c (K) from EPR : magnetic ground state	T_c (K) from EPR : non-magnetic ground state	T_c' : superconductive transition
—	—	—	—	—	—
1	0.2 ± 0.1				0.8
2	0.5 ± 0.1		11		0.2 (?)
3	2 ± 0.3	11.5-14.5	14		
4	4 ± 0.7	9 -15	10		
5	6.5 ± 0.5	14 -18	—	13	
6	30 ± 5	14 -26	—	13	

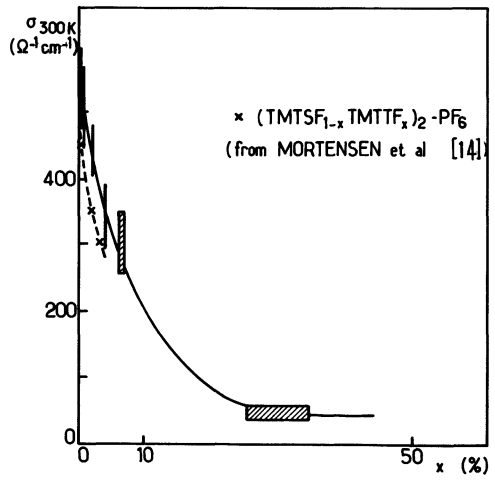

Fig. 1. — x dependence of the room temperature value of σ'' (the rectangles represent the estimated uncertainties). The crosses correspond to the data obtained for PF_6 alloys by Mortensen *et al.* [4].

been disturbed by erratic jumps of resistance and it has been impossible to get full temperature curves. The same behaviour was already observed with pure TMTTF or TMTSF salts [9, 16]. However we have obtained reproducible results when cooling slowly the samples below 50 K using different crystals issued from the same batch. For this reason, we have normalized the resistance temperature dependence at 50 K. These experimental results are given in figure 2. A metal-insulator transition appears for each compound. A very weak effect is seen for the first alloy, its strength is enhanced with increasing TMTTF doping. The alloys (1) and (2) exhibit a reproducible reentrant metallic behaviour below 1 K.

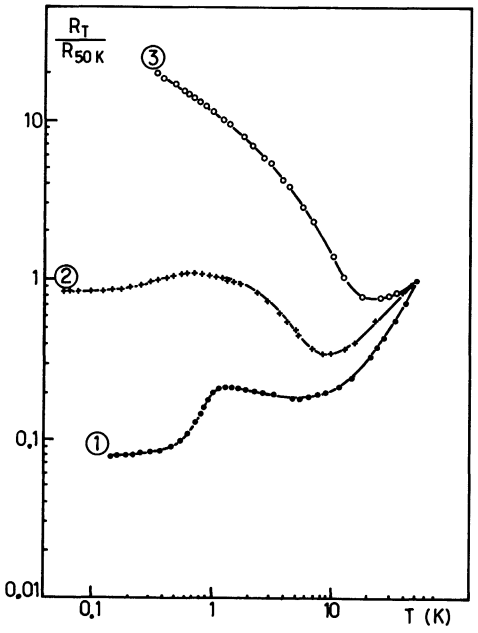

Fig. 2. — Very low temperature resistivity of three alloys (x = 0.2, 0.5 and 2 %).

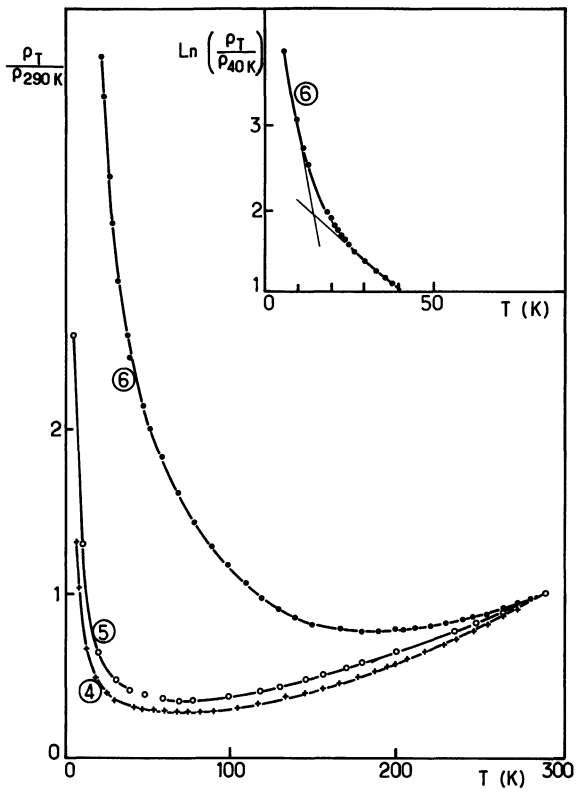

Fig. 3. — Reduced temperature dependences of the resistivity for three alloys : + crosses for x = 4 %; ○ open circles for x = 6.5 %; ● dots for x = 30 % (low T resistivity is given in insert).

For the alloys (4), (5) and (6) it has been possible to get continuous curves in the temperature range 6-300 K. Thus, the brittleness of the samples seems to decrease with doping. The corresponding temperature dependences are given in figure 3. A metal-insulator transition appears at low temperature in the three cases. The alloys (4) and (5) show a metallic behaviour in a large temperature range. On the contrary, a broad minimum is observed for the 30 % doped sample, whose behaviour is similar to that of the TMTTF salts [9].

2.2 EPR EXPERIMENTS. — The EPR experiments have been carried out with an X band spectrometer (VARIAN 4500) equipped with a helium gas flow accessory. Every measurement has been done on single crystals. For this reason, on most of the alloys, we were not able to detect a resonance line at room temperature and a complete set of experimental data was obtained only below 100 K when the line narrows enough. It should be noted that the shape of the resonance lines are always Lorentzian : neither a Dysonian line nor a broadening effect due to an inhomogeneous sample was observed.

We have systematically investigated the linewidth and the g-factor for the most interesting position of the sample, namely when the needle axis is parallel to the applied static magnetic field. They are reported

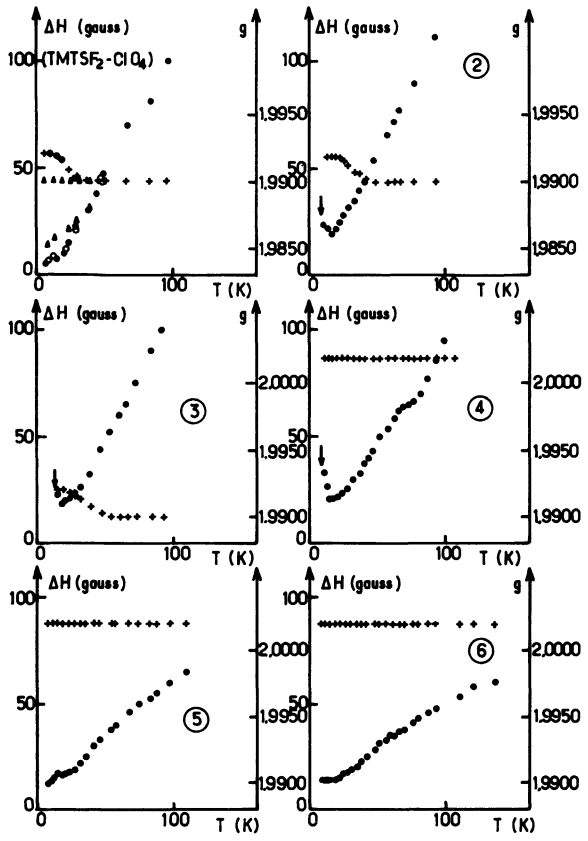

Fig. 4. — EPR data : x components of the linewidth (ΔH) and the g-factor tensors (the needle axis of the crystal is parallel to the static magnetic field). These results are presented for pure $TMTSF_2$-ClO_4 and for the different alloys (numbers 2 to 6). For the $TMTSF_2$-ClO_4 crystal (upper left figure) two different temperature cycles have been carried out below 40 K : — slow cooling and heating rates (respective symbols for the g-factor (+, ●) and the linewidth (●, ○)); — a quenching followed by a slow heating rate (g-factor (△), linewidth (▲)).

and compared to the corresponding quantities for the pure TMTSF sample in figure 4. The linewidth first decreases with decreasing temperature. Then, the behaviour depends on the value of x. For x small (samples (2), (3), (4)), the linewidth increases at low temperature and the resonance line becomes undetectable below a given temperature indicated by an arrow in figure 4. For larger values of x, we observe either a bump (sample (5)) or simply a plateau (sample (6)).

The corresponding g value (g_{xx}) is also sensitive to the amount of doping :

— for the pure TMTSF salt and for the lightest doped samples, its temperature dependence is sensitive to the cooling rate of the crystal. For a slow cooling rate (~ 40 K/hour) the g_{xx} component is temperature independent down to 40 K ; then, below this temperature range the g_{xx} value increases and saturates [16]. This effect is reversible when the heating cycle is accomplished up to 40 K. On the contrary a sample quenching by a fast cooling (from 40 K to 8 K is a few seconds) gives a constant value for the line position without any step as previously observed; by heating up the crystal slowly at different temperatures this behaviour is confirmed. At the same time the resonance line is enlarged below 40 K compared with the former temperature dependence for a slow cooling rate (see Fig. 4);

— for higher values of x, we observe a temperature independent g value similar to that observed in the TMTTF series [9].

Concerning samples (5) and (6), we also give in figure 5*a* the paramagnetic susceptibility as obtained by the integration of the EPR resonance line.

The linewidth anisotropy is small for all the alloys and similar to the pure compound observation [16]. Therefore we do not present the temperature dependence of the two other components of the linewidth tensors. The corresponding components of the g tensor are nearly constant over all the temperature range 6-100 K, so we tabulate their values at 100 K (Table II) in which they are compared with g_{xx} at the same temperature (we also give the related values for the two pure samples). They are presented in figure 5*b* where the same cross-over between two different behaviour is detected at $x \simeq 0.05$. Finally we

Table II. — *Principal components of the second rank g tensor measured at* 100 K *and mean value of the square of the g factor anisotropy* ($\delta g_{ii} = g_{ii} - 2.0023$). *The x axis is the direction of the conductive chains. The y and z directions are transverse directions corresponding to the g-extrema.*

Samples $(TMTTF_xTMTSF_{1-x})_2ClO_4$	g_{xx} $H_0 /\!/ a^*$	g_{zz} $H_0 /\!/ c^*$	g_{yy} $H_0 /\!/ b^*$	$\overline{\Delta g^2} = \frac{1}{3}(\Delta g_{xx}^2 + \Delta g_{yy}^2 + \Delta g_{zz}^2)$
$x = 0$ $(TMTSF)_2ClO_4$	1.990 0	2.030 4	2.039 4	7.50×10^{-4}
(2) $x = 0.005$	1.990 0	2.030 2	2.035 0	6.66×10^{-4}
(3) $x = 0.02$	1.990 0	2.030 1	2.033 5	6.49×10^{-4}
(4) $x = 0.04$	2.001 8	2.028 0	2.032 0	5.14×10^{-4}
(5) $x = 0.065$	2.002 0	2.023 5	2.029 0	3.87×10^{-4}
(6) $x = 0.30$	2.002 0	2.018 4	2.022 0	2.16×10^{-4}
$x = 1$ $(TMTTF)_2ClO_4$	2.002 1	2.009 0	2.011 1	0.408×10^{-4}

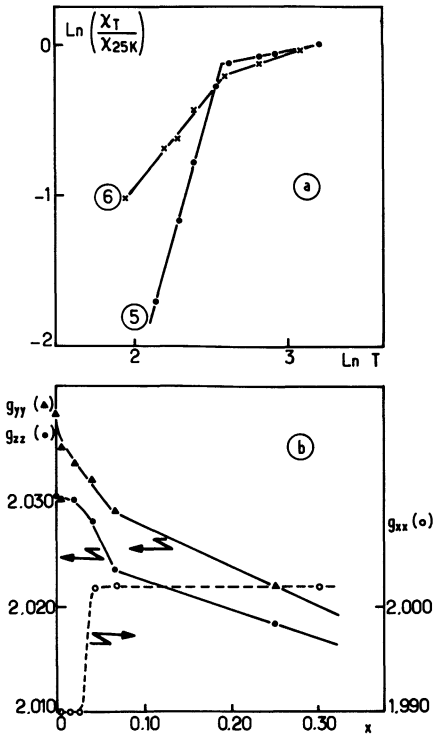

Fig. 5. — *a*) EPR paramagnetic susceptibility in a Log-Log plot for the samples (5) and (6). *b*) x dependence of the g factor components (g_{xx}, g_{yy}, g_{zz}) (see the definition of these quantities in the text).

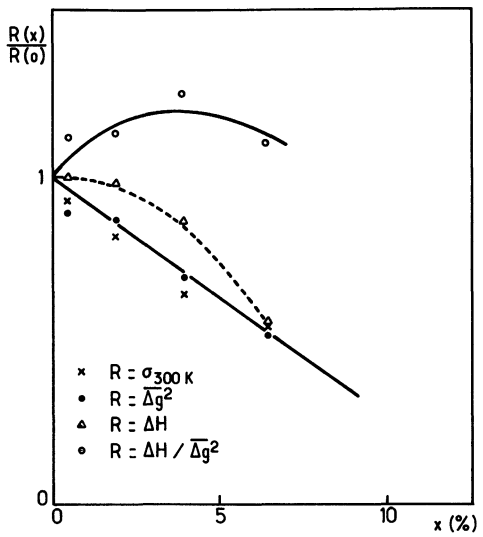

Fig. 6. — x dependence of the following reduced quantities R : σ_{300K}, $\overline{\Delta g}^2$, ΔH and $\Delta H/\overline{\Delta g}^2$.

also give in table II the square of the g-factor anisotropy usually defined by :

$$\overline{\Delta g}^2 = \tfrac{1}{3}[\Delta g_{xx}^2 + \Delta g_{yy}^2 + \Delta g_{zz}^2]$$

where

$$\Delta g_{ii} = g_{ii} - g_e$$

g_e is the free electron g value.

These results are consistent with those obtained for the PF_6 alloys [12].

3. **Discussion of the experimental results.** — 3.1 THE METALLIC STATE. — The comparison of the electrical and EPR results for the different samples enables a discussion of the effect of doping in the metallic state (mainly for the small values of x) to be made.

As already mentioned we observe a drastic effect of the doping on the electrical conductivity (σ_{300K}) and on the g-factor and linewidth (ΔH) components at 100 K. A similar effect has already been reported for σ and g in the case of the PF_6 alloys [14]. To compare all the experimental data we have plotted in the same figure the different reduced properties

$$R_n(x) = \frac{R(x)}{R(x=0)}$$

where R is respectively σ_{300K}, $\overline{\Delta g}^2_{100K}$ or ΔH_{100K}.

As is usually done to compare different doped samples [17], we have also given the reduced linewidth dependence $\gamma = \Delta H/\overline{\Delta g}^2$ in figure 6. By doing this we take account of the linewidth changes (see Fig. 4) with the alloy compositions which are due to the effective spin-orbit coupling variations (the Se atom has a larger spin-orbit coupling than the S atom because of a higher atomic number).

At a first evidence there is no drastic effect on γ which is nearly constant for light doping with TMTTF. This indicates a small dependence of the spin-flip matrix element on x and a spin-lattice relaxation time quite similar to the expected value found on $(TMTSF)_2ClO_4$ and similar radical cation salts [18] in this medium temperature range.

In contrast the similar decreases of $\overline{\Delta g}^2$ and σ_{300K} are about 8 times larger than the expected linear extrapolation between $x = 0$ and $x = 1$. This result, in agreement with the work of Mortensen *et al.* [14] cannot at present be explained. However, it should be noted that the longitudinal conductivity of the sample (6) is similar to that of $(TMTTF)_2ClO_4$. As already proposed for the TMTTF salts [9], this peculiar behaviour of $\sigma(T)$ (low absolute value and high temperature maximum of the conductivity) could be due to a localization process probably enhanced by the doping effect. It should be mentioned that this process receives a very simple explanation with the Emery *et al.* theory [12]. From their point of view, this localization due to the growth of a $4\,k_F$ CDW is an intrinsic property of the conducting chains.

The most attractive result is given by figure 5. We observe a cross-over between two different behaviours for a well-defined value of doping amount. For light alloys the temperature dependence of g_{xx} is particularly striking. Takahashi *et al.* [19] have recently reported NMR experiments which show for $(TMTSF)_2ClO_4$ the possibility of a quenched state for a fast cooling of the sample. Shirane and Pouget [20] have shown by structural experiments that an

ordering of the anions occurs in this compound when the temperature is lowered smoothly. The wavevector component along the a axis of the associated superstructure is different from the $2\,k_F$ value and this ordering does not drive the compound into an insulating state. We think that the temperature dependence of g_{xx} is the consequence of this phase transition while a fast cooling freezes in a lattice disorder the perchlorate anions [20] and the g-factor stays temperature independent. It is noteworthy to indicate that this g-factor effect exists for the lightest doped samples only. For $x > 5\,\%$ the disordered state might be thermodynamically stable and in the same time the g-factor increases suddenly to the value observed for the TMTTF salts [9].

To conclude this part, we can note that the doping process is a good experimental parameter to study the metallic state of the TMTSF salts. We are going to see in the following that this parameter is also relevant for elaborating the phase diagram.

3.2 THE PHASE DIAGRAM. — We now discuss the effect of doping on the different low temperature instabilities. This discussion implies that we are looking for the intrinsic properties of the electronic chains. In other words, we assume that there is no order-disorder phase transition with the wavevector component $2\,k_F$ as in pure $(TMTTF)_2ClO_4$. This is in agreement with preliminary X-ray data [20]. Furthermore the physical properties, and in particular the EPR linewidth, behave differently when such a transition is detected (see for example the behaviour of $(TMTTF)_2ClO_4$ in [9]).

There are only three possible low temperature intrinsic ground states. The first one is the superconductive state which has been described in the TMTSF series [1]. The others are both associated with the condensation of insulating ground states but exhibiting a very different nature. The first one gives the SDW state whose magnetic nature has been clearly established [18]. One of the experimental evidences of this instability is the occurrence of an antiferromagnetic resonance (AFMR) beyond the phase transition [21]. This special type of resonance which is due to the occurrence of the internal staggered field below the phase transition is usually observed in inorganic antiferromagnetic materials [22]. For this reason the EPR signal is not detectable at the usual g value with a conventional spectrometer. The second one gives the insulating ground state as observed for some TMTTF salts when no counterion effect is involved in the phase transition mechanism [9]. This state is non magnetic and has been described as a SP state [12]. The usual EPR signal is seen below the transition temperature and the corresponding paramagnetic susceptibility obtained by integration of the resonance signal follows an activation law.

From our experimental data, we can deduce the experimental phase diagram. First, we note that we observe a cross-over between two different insulating ground states at $x \simeq 5\,\%$. The first state ($x < 5\,\%$) is similar to the magnetic SDW phase of the TMTSF salts. For exemple, the EPR signal is not detected below the transition. For the second state ($x > 5\,\%$), the low temperature behaviour of the EPR linewidth and the paramagnetic susceptibility is similar to that observed in the TMTTF series and we assume that this ground state is non magnetic as for $(TMTTF)_2PF_6$. New X-ray experiments would be useful to confirm this point.

To estimate the temperature (T_c) of the different transitions, one can use either the conductivity or the EPR results :

— The maximum of the $\dfrac{d(\mathrm{Ln}\,\sigma)}{d(1/T)}$ *versus* T plot usually gives T_c. However, in this case the determination is not very accurate because of the broadening effect of the doping agent and only an estimate of T_c is given by this method. The corresponding values are reported in table I.

— Another determination is possible using the EPR properties. When a SDW condensation occurs, T_c can be identified as the temperature when the resonance line disappears. These temperatures are indicated by arrows on figure 4. When a non-magnetic ground state occurs (samples (5) and (6)) we have estimated T_c using the temperature dependence of the paramagnetic susceptibility. As usually found, a change in the slope of the Ln χ *versus* Ln T plot gives an accurate determination of T_c (Fig. 5*a*). All these temperatures are given in table I.

The superconductive instability is only visible on samples (1) and (2). For the first sample, a superconductive transition is observed at $T_c \simeq 800$ mK. The second sample gives a smooth decrease of $\rho(T)$ at a very low temperature (see Fig. 3). This behaviour could be related to the onset of a superconducting ground state for an inhomogeneous sample as already observed for irradiated samples [23]. It should be mentioned nevertheless that the same result is found if we observe a reentrant metallic phase below 700 mK. This unusual recovery of the high symmetry metallic phase below the condensation of the lower symmetrical SDW phase could be due to the competition between the superconductive and SDW instabilities. These fluctuations, inducing a reentrant behaviour, have been shown to exist in a quasi 1d theoretical model [24]. Because of the lack of experimental data at very low temperature it seems very hard to choose between these two models. However, the superconductive instability is clearly very sensitive to the doping. A more complete discussion about this point, which will imply high pressure results, will be given in the following paper.

The end of this discussion will be devoted to the competition between the two different insulating ground states. As already mentioned, we observe a

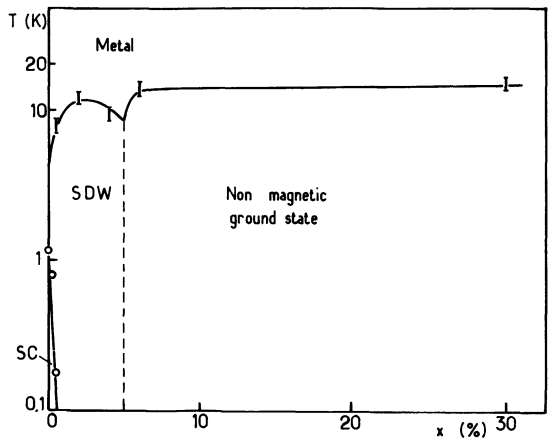

Fig. 7. — Deduced experimental phase diagram for $(TMTSF_{1-x}TMTTF_x)_2$-ClO_4 alloys.

cross-over between a SDW to a non-magnetic low temperature ground state for $x \simeq 5\ \%$.

Using the values of the transition temperatures given in table I, we can construct the experimental phase diagram in the plane (T, x) which is given on figure 7. To discuss more quantitatively our experimental results we will illustrate the competition between the two different ground states with a very simple Landau model.

3.3 A SIMPLE MODEL FOR THE SP-SDW COMPETITION. — Following Emery *et al.* [12] we will assume that the observed phase diagram results from the competition between a SDW and a SP ground state. To illustrate this theory and to give a correspondence between the experimental and theoretical parameters, we will construct a very simple Landau model.

The SP phase is characterized by the lattice modulation ρ which can be used as an order parameter. The order parameter of the SDW is the spin modulation σ.

The most general Landau energy describing the competition between ρ and σ reads :

$$\Delta F_1 = \frac{A_1}{2} |\rho|^2 + \frac{A_2}{2} |\sigma|^2 + \frac{B_{11}}{4} |\rho|^4 + \frac{B_{22}}{4} |\sigma|^4 + \frac{B_{12}}{2} |\sigma|^2 |\rho|^2 .$$

As is usually done, A_1 and A_2 are assumed to be the only temperature dependent coefficients and $A_i = A_i'(T - T_i)(i = 1 \text{ or } 2)$.

A simultaneous ρ and σ ordering is supposed to be excluded and we will choose $B_{12} > \sqrt{B_{11} B_{22}}$ (B_{11} and B_{22} are assumed to be positive).

According to the Emery *et al.* description of the SDW-SP competition [12], the coupling with the possible 4 k_F CDW must be introduced. This coupling term reads :

$$\Delta F_2 = - \lambda |\rho|^2 |\rho_{4k_F}|$$

where λ is a positive coupling constant.

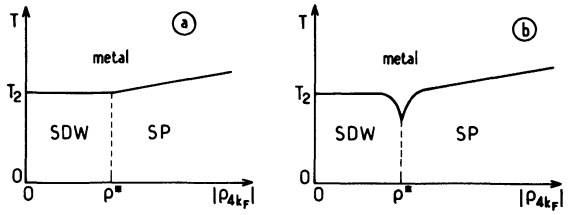

Fig. 8. — *a*) Mean field theoretical phase diagram corresponding to the model described in the text (the vertical line is a particular case when $A_1' = A_2' \sqrt{\frac{B_{11}}{B_{22}}}$). *b*) Theoretical phase diagram for the same model including fluctuations of the order parameters.

The negative sign comes from the minimization of the ρ phase.

Then, the free energy describing the SDW-SP cross-over is :

$$\Delta F = \Delta F_1 + \Delta F_2 .$$

To observe a SDW ground state when $\rho_{4k_F} = 0$ (TMTSF salts limit) we will assume that $T_2 > T_1$.

A typical theoretical phase diagram obtained with this model is given in the $T, |\rho_{4k_F}|$ plane in figure 8*a*. The cross-over occurs at a critical value ρ^* of $|\rho_{4k_F}|$ given by :

$$\rho^* = \frac{A_1'}{2\lambda} \left(\frac{B_{22}}{B_{11}}\right)^{1/4} (T_2 - T_1) .$$

The metal-SDW transition temperature is T_2 which is considered as constant in the model. The slope of the metal-SP transition line is simply $\frac{2\lambda}{A_1'} \left(\frac{B_{11}}{B_{22}}\right)^{1/4}$.

An improvement of this mean field phase diagram needs the introduction of fluctuations of the order parameters. It is well known that this effect will be particularly important near ρ^*. In this part of the phase diagram, a lowering of the ordering temperature is expected to give the phase diagram of figure 8*b* [24, 25].

Using the prevision of the model, a comparison can be made with the experimental results. Of course, the superconductive instability has not been introduced in the model and a discussion of the shape of the experimental phase diagram cannot be made, using this model, for very weak values of $x (x < 2\ \%)$.

The experimental phase diagram given in figure 7 is clearly similar to the theoretical diagram of figure 8*b* if we assume that x is the experimental parameter corresponding to $|\rho_{4k_F}|$. With this assumption, several experimental results are clarified :

First, the x dependence of the room temperature conductivity can be explained : the increase of $|\rho_{4k_F}|$ with doping is equivalent to a localization which strongly reduces the mean free path of the electrons. At the same time, a maximum of conductivity occurs at higher temperature. Note that $|\rho_{4k_F}|$ is mainly, at

least for small values of x, an intrachain parameter; the interchain couplings are not expected to change drastically for a small amount of TMTTF. On the contrary, a change of the molecular orbitals is evidenced by the behaviour of the g-factor components at the cross-over ($x \simeq 5\,\%$). This remark has to be related with the « bond model » proposed by Wudl [26]. According to this model, the SDW instability in the TMTSF series is due to the properties of the orbitals of the TMTSF molecules.

Then, the slope of the metal-SP transition line is expected to be small : λ which is a coupling constant must be small compared with $A_1' T_2$, and the transition temperature is expected to be almost the same even for large variations of $| \rho_{4k_F} |$. This explains why all the intrinsic phase transitions (when an ordering of the non-centrosymmetric anions does not exist) occur in the same temperature range either for the TMTTF or the TMTSF salts.

4. **Conclusion.** — We have studied

$$(TMTSF_{1-x}TMTTF_x)_2ClO_4$$

alloys (for $x \leqslant 0.30$) prepared electrochemically. Both the electrical conductivity, the EPR linewidth and the g-factor are drastically affected by substitution of TMTTF inside the TMTSF stacks. This behaviour is in agreement with the properties of the isomorphous solid solutions of PF_6 salts [14].

The low temperature data reveal a very attractive phase diagram. The superconductive state disappears very quickly with doping. A more complete discussion about this point including high pressure results will be presented in the second part of this work.

Moreover, a cross-over from a magnetic to a non-magnetic insulating ground state is observed for $x \simeq 5\,\%$. This behaviour has been related to the theory of Emery *et al.* To illustrate their main results and to give the relation between the theoretical and the experimental parameters, we have constructed the Landau model corresponding to their microscopic theory. This model allows an understanding to be obtained of the drastic effects of a small amount of doping as the result of a localization process. This process is expected to change (at least, for small values of x) essentially the symmetry of the molecular orbitals (see g-factor results) without any large variation of the interchain couplings. At the same time, the metal-insulator transition temperature is shown to be almost a constant, in agreement with the experimental data.

Finally, it should be mentioned that the role of a counterion ordering with a wave vector component at $2\,k_F$ has not been investigated in this paper. The preparation and the study of samples rich in TMTTF ($x > 0.3$) could be useful to completely obtain the phase diagram.

Acknowledgments. — We are grateful to J. P. Pouget, S. S. P. Parkin and J. Prost for fruitful discussions. We also thank T. Takahashi, F. Creuzet and D. Jérôme for communication of their manuscript.

References

[1] Jerome, D., Mazaud, A., Ribault, M. and Bechgaard, K., *J. Physique-Lett.* **41** (1980) L-95.

[2] Bechgaard, K., Jacobsen, C. S., Mortensen, K., Pedersen, H. J. and Thorup, N., *Solid State Commun.* **33** (1980) 1119.

[3] Pouget, J. P., Moret, R., Comes, R. and Bechgaard, K., *J. Physique Lett.* **42** (1981) L-543.

[4] Parkin, S. S. P., Jerome, D. and Bechgaard, K., Proceedings of the International Conference of low dimensional Conductors (Boulder, Colorado August 1981) *Mol. Cryst. Liq. Cryst.* **79** (1982) 569.

[5] Pouget, J. P., Moret, R., Comes, R., Bechgaard, K., Fabre, J. M. and Giral, L., *Physica* **108B** (1981) 1187.

[6] Jerome, D., Proceedings of the International Conference on low dimensional Conductors (Boulder, Colorado August 1981) *Mol. Cryst. Liq. Cryst.* **79** (1982) 511.

[7] Galigne, J. L., Liautard, B., Peytavin, S., Brun, G., Maurin, M., Fabre, J. M., Torreilles, E. and Giral, L., *Acta Crystallogr.* **B 35** (1979) 2609.

[8] Delhaes, P., Coulon, C., Amiell, J., Flandrois, S., Torreilles, E., Fabre, J. M. and Giral, L., *Mol. Cryst. Liq. Cryst.* **50** (1979) 43.

[9] Coulon, C., Delhaes, P., Flandrois, S., Lagnier, R., Bonjour, E. and Fabre, J. M., *J. Physique* **43** (1982) 1059.

[10] Creuzet, F., Takahashi, T., Jerome, D. and Fabre, J. M., To be published.

[11] Parkin, S. S. P., Scott, J. C., Torrance, J. B., Engler, E. M., To be published.

[12] Emery, V. J., Bruinsma, R., Barisic, S., *Phys. Rev. Lett.* **48** (1982) 1039.

[13] Parkin, S. S. P., Creuzet, F., Ribault, M., Jerome, D., Bechgaard, K. and Fabre, J. M., International Conference on low dimensional conductors (Boulder, Colorado August 1981) *Mol. Cryst. Liq. Cryst.* **79** (1982) 605.

[14] Mortensen, K., Tomkiewicz, Y., Schultz, T. D., Engler, E. M., Patel, V. V. and Taranko, A. R., *Solid State Commun.* **40** (1981) 915 and private communication.

[15] Chasseau, D., Hauw, C. and Gaultier, J., Private communication.

[16] Delhaes, P., Amiell, J., Manceau, J. P., Keryer, G., Flandrois, S., Fabre, J. M. and Giral, L., *C.R. Hebd. Séan. Acad. Sci. Paris* **293** (1981) 347.

[17] Tomkiewicz, Y., Engler, E. M. and Schultz, T. D., *Phys. Rev. Lett.* **35** (1975) 456.

[18] Scott, J. C., Pederson, H. J. and Bechgaard, K., *Phys. Rev. Lett.* **45** (1980) 125.

[19] Takahashi, T., Jerome, D., Bechgaard, K., *J. Physique-Lett.* **43** (1982) L-565.

[20] SHIRANE, G., POUGET, J. P., Private communication (work in progress).

[21] TORRANCE, J. B., PEDERSEN, H. J. and BECHGAARD, K., *Bull. Am. Phys. Soc.* (communication AH 3) March 1982, p. 150.

[22] See for example : HERPIN, A., *Théorie du magnétisme.* Bibliothèque des sciences et techniques nucléaires (Presses Universitaires de France) 1968a, p. 562.

[23] BOUFFARD, S., CHIPAUX, R., JEROME, D. and BECHGAARD, K., *Solid State Commun.* **37** (1981) 405.

[24] COULON, C. and PROST, J., *J. Physique-Lett.* **42** (1981) L-241.

[25] FISHER, M. E., NELSON, D. R., *Phys. Rev. Lett.* **32** (1974) 1350 ;
BANAVAR, J. R., JASNOW, D., LANDAU, D. P., *Phys. Rev.* **B 20** (1979) 3820.

[26] WUDL, F., *J. Am. Chem. Soc.* **103** (1981) 7064.